Parasitic Inclinations in Cable-Driven Parallel Robots using Cable Loops

Saman Lessanibahri, Philippe Cardou, Stéphane Caro

Available online at www.sciencedirect.com

ScienceDirect

Procedia CIRP 70 (2018) 296–301

www.elsevier.com/locate/procedia

28th CIRP Design Conference, May 2018, Nantes, France

Parasitic Inclinations in Cable-Driven Parallel Robots using Cable Loops

Saman Lessanibahri[a], Philippe Cardou[b], Stéphane Caro[c]

[a]Centrale Nantes, Laboratoire des Sciences du Numérique de Nantes, UMR CNRS 6004, 1, rue de la Noë, 44321 Nantes, France
[b]Laboratoire de robotique, Département de génie mécanique, Université Laval, Québec, QC, Canada
[c]CNRS, Laboratoire des Sciences du Numérique de Nantes, UMR CNRS 6004, 1, rue de la Noë, 44321 Nantes, France

* Corresponding author. Tel.: +33-240-376-925; fax: +33-240-376-925. *E-mail address:* Saman.Lessanibahri@ls2n.fr

Abstract

Cable-Driven Parallel Robots (CDPRs) also noted as wire-driven robots are parallel manipulators with flexible cables instead of rigid links. A CDPR consists in a base frame, a Moving-Platform (MP) and a set of cables connecting in parallel the MP to the base frame. CDPRs are well-known for their advantages over the classical parallel robots in terms of large workspace, reconfigurability, large payload capacity and high dynamic performance. In spite of all the mentioned advantages, one of the main shortcomings of the CDPRs is their limited orientation workspace. The latter drawback is mainly due to cable interferences and collisions between cables and surrounding environment. Hence, a planar four-Degree-of-Freedom (DoF) under-constrained CDPR with an articulated MP is introduced and studied in this paper. The end-effector is articulated through a cable loop, which enables the robot to obtain a modular pose determination, namely orientation and positioning. As a result, the mechanism under study has an unlimited and singularity-free orientation workspace in addition to a large translational workspace. It should be noted that some unwanted rotational motions of the moving platform, namely, parasitic inclinations, arise due to the cable loop. Finally, those parasitic inclinations are modeled and assessed for the mechanism at hand.

Peer-review under responsibility of the scientific committee of the 28th CIRP Design Conference 2018.

Keywords: Cable-Driven Parallel Robots, Cable Loop, Kinematics, Large Workspace;

1. Introduction

One advantage of cable-driven parallel robots that has not yet been fully exploited is the possibility of using the cables to transmit power directly from motor fixed to the frame to the moving platform. This power can then be used to actuate a tool or to control additional degrees of freedom such as rotations over wide ranges [14], for example. In this article, we study the simplest expression of a bi-actuated cable circuit, namely, a cable loop, for controlling rotations of the CDPR end effector over wide ranges. The cable making the cable loop connects two actuators through two fixed pulleys located at CDPR exit points, A_i and A_{i+1} while it is coiled around a drum attached to the MP. Figure 1 illustrates a CDPR prototype introduced in this paper and employing a cable loop. This architecture provides an unlimited orientation workspace of the MP and consequently, the following two motions are generated. Translation for identical motions of the actuators, and pure rotation that corresponds to the case while two actuators rotate in reverse directions. The concept of cable loop is detailed in [14]. In general, by using a cable loop in a CDPR, the translational motions of the MP lead to equal cable tensions on both sides of the drum. Furthermore, the pure rotation of the end-effector is a result of the different tensions generated by two actuators. The cable loop allows us to enlarge the orientation workspace of the manipulator at hand, but there exists an undesired rotation associated to the rotation of the MP while different tensions applied on the cable loops by the two actuators. Employing cable loops in the design of the CDPRs has been the subject of some previous works, e.g. [8,9,12]. Nevertheless, to the best of the authors' knowledge, the parasitic inclination induced by cable loops has not been addressed up to now. Therefore, the main contribution of this paper lies in the modeling and evaluation of parasitic inclinations in CDPRs containing one cable loop.

Two approaches are described in the paper to determine the orientation of the articulated MP and as a consequence its parasitic inclinations. The first approach aims at solving the geometrico-static model of the CDPR at hand, to find the orientation of the MP for a given position of its geometric center. Carricato [2] studied an analogous problem namely, inverse geometrico-static problem of under-constrained CDPRs which poses major challenges due to the coupling between geometry and static-equilibrium of under-constrained CDPRs. The second approach aims at approximating the orientation of the MP without considering the geometrico-static model of the manipulator, but by using some geometric properties of the cable loop and the artic-

2212-8271
Peer-review under responsibility of the scientific committee of the 28th CIRP Design Conference 2018.
10.1016/j.procir.2018.02.013

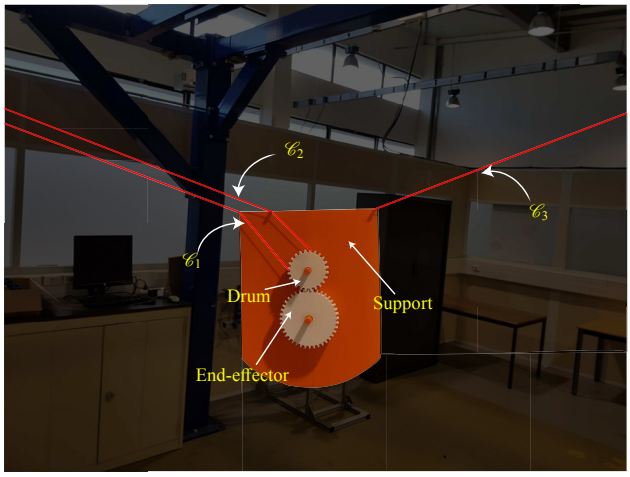

Fig. 1: Articulated MP of a planar CDPR containing a cable loop

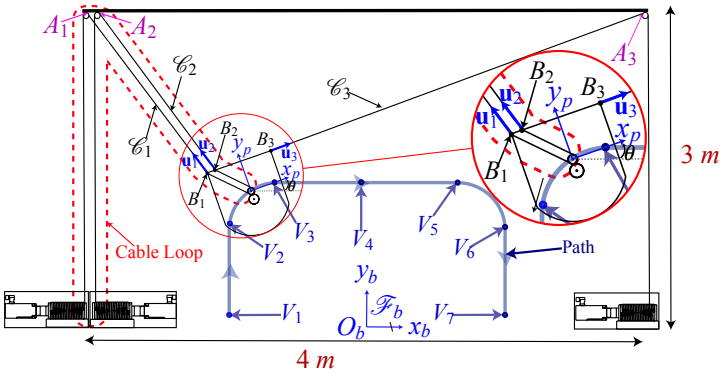

Fig. 2: A four-DoF planar cable-driven parallel robot with a cable loop

ulated MP. Finally, the results obtained by the two approaches for a planar CDPR with one cable loop are compared.

The paper is organized into eight sections. Section 2 describes the articulated MP of the planar CDPR under study. Section 3 details the geometrico-static model of the CDPR with a cable loop. Section 4 presents two approaches to find the orientation of the MP. Section 5 introduces a method to assess the parasitic inclination of the planar CDPR with one cable loop. The parasitic inclination for a case study is presented in section 6 and the discussion is detailed in section 7. Finally, the last section concludes the paper.

2. Description of the Manipulator under Study

This section describes the manipulator under study. This manipulator has a planar workspace with an articulated MP which can host different types of end-effectors with one DoF. The overall manipulator consists in a base frame and two actuated cables connecting in parallel the articulated MP to the base frame as shown in figure 2. The planar manipulator possesses four-DoF while, it is actuated by three motors through two cables. Therefore, the manipulator is considered under-actuated. The MP has two translation DoF in the $\mathbf{x}O\mathbf{y}$ plane, one rotational DoF perpendicular to its translation plane. The actuation of the additional degree of freedom on the moving platform is done through a cable loop and a drum, so that no motor needs to be mounted on the moving platform. The objective of this manipulator is to provide the underlying foundation for investigating the parasitic inclinations induced by cable loops in CDPRs.

Figure 1 illustrates the articulated MP of the CDPR under study. This MP is composed of a support, a drum and an end-effector. The support forms the overall body of the moving-platform and accommodates cable anchor points (B_1, B_2, B_3) and other components. The drum operates the end-effector through the cable loop. Both the drum and the end-effector are gears such that the rotational motion of the end-effector is provided by the rotational motion of the drum. A cable (cable loop) connected to two actuators, which are not shown in Fig. 1, is wounded about the drum to make the latter rotate about its own axis. The left side of this cable is denoted $\mathscr{C}_1$ whereas its right side is denoted $\mathscr{C}_2$. Another cable, named $\mathscr{C}_3$, is connected to both the support of the articulated MP and a third actuator. The cable loop consists in two segments each with independent cable tension (t_1 and t_2). First segment, $\mathscr{C}_1$, is composed of the part of the cable loop which connects the first motor to the drum through points A_1 and B_1. The second segment is denoted as $\mathscr{C}_2$ and connects the second motor to the drum through points A_2 and B_2.

3. Geometrico-Static Model of a Planar CDPR with a Cable Loop

This section presents the mathematical model of the planar four-DoF under-constrained CDPR shown in Fig. 2. The considered robot is actuated by three motors. This model defines robot geometric model along with its static equilibrium equation. Since the geometry and the statics of under-constrained CDPRs are coupled, they should be solved simultaneously. Accordingly, the loop-closure and static equilibrium equations of the CDPR are written in order to obtain its geometrico-static model of the planar CDPR under study. The three following equations express the loop-closure equations of the manipulator at hand.

$$ {}^b\mathbf{l}_i = {}^b\mathbf{a}_i - {}^b\mathbf{p} - {}^b\mathbf{R}_p\, {}^p\mathbf{b}_i, \quad i = 1,\ 2,\ 3 \tag{1} $$

where ${}^b\mathbf{l}_i$ is the i-th cable vector, i.e., the coordinate vectors pointing from point B_i to point A_i. ${}^b\mathbf{a}_i = [a_{ix},\ a_{iy}]^T$, ${}^p\mathbf{b}_i = [b_{ix},\ b_{iy}]^T$ and ${}^b\mathbf{p} = [p_x,\ p_y]^T$ are the Cartesian vector of points A_i, B_i and P, respectively, expressed in frame $\mathscr{F}_b$. ${}^b\mathbf{R}_p$ is the rotation matrix associated to the rotation of $\mathscr{F}_p$ with respect to $\mathscr{F}_b$ and is expressed as follows:

$$ {}^b\mathbf{R}_p = \begin{bmatrix} \cos\theta & -\sin\theta \\ \sin\theta & \cos\theta \end{bmatrix} \tag{2} $$

$\theta = \angle(\mathbf{x}_b,\ \mathbf{x}_p)$ defines the orientation of the MP. $\mathbf{t}_i,\ i = 1,\ 2,\ 3$ is the i-th cable tension vector and it is directed from B_i toward the exit point A_i. $\mathbf{t}_i = t_i\, {}^b\mathbf{u}_i$ and its magnitude is expressed as $t_i = \|\mathbf{t}_i\|_2,\ i = 1,\ 2,\ 3$ and ${}^b\mathbf{u}_i$ is denoted as the i-th cable unit vetor. In order to compute the unit cable vector, ${}^b\mathbf{u}_i$, we normalize, ${}^b\mathbf{l}_i$ as follows:

$$ \mathbf{u}_i = \frac{\mathbf{l}_i}{l_i}, \quad i = 1,\ 2,\ 3 \tag{3} $$

l_i being the i th cable length. The following set Σ is introduced, $\Sigma = \Sigma_1 + \Sigma_2 + \Sigma_3 + \mathscr{C}_1 + \mathscr{C}_2 + \mathscr{C}_3$, which gathers the isolated parts of the robots in order to analyze its static equilibrium. Σ_1, Σ_2 and

Σ_3 stand for end-effector, drum and support, respectively. From Fig. 3, the external wrenches exerted on Σ are cable tensions, $\mathbf{t}_i$, $i = 1, 2, 3$, the weight of the MP, $m\mathbf{g}$, and the frictional moment or the resistance to relative motions between Σ_1 and Σ_2 that is denoted as m_{fr}.

The equilibrium of the external forces applied onto Σ, is expressed as follows:

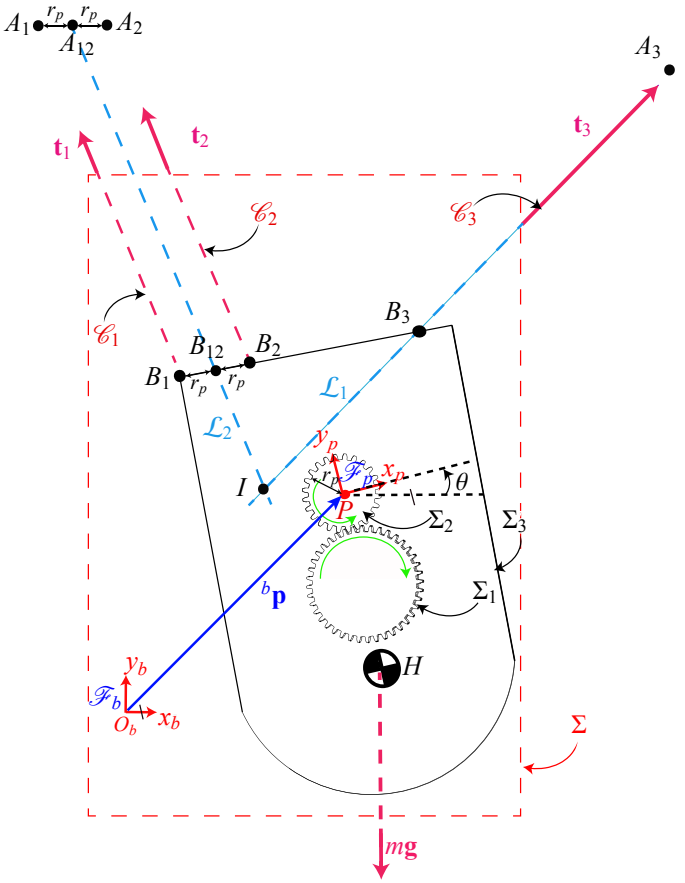

Fig. 3: Moving-platform of the four-DoF planar under-constrained cable-driven parallel robot

$$\sum_{i=1}^{3} t_i {}^b\mathbf{u}_i + m\mathbf{g} = 0 \tag{4}$$

In Eq. (4), m is the mass of the MP and $\mathbf{g} = [0, -g]^T$ is the gravity acceleration with $g = 9.81\ m.s^{-2}$. The equilibrium of moments about point P in frame $\mathscr{F}_b$ is expressed as follows:

$$\sum_{i=1}^{3} \left(\left({}^b\mathbf{b}_i - {}^b\mathbf{p} \right)^T \mathbf{E}^T \mathbf{t}_i \right) + \left({}^b\mathbf{h} - {}^b\mathbf{p} \right)^T \mathbf{E}^T m\mathbf{g} = 0 \tag{5}$$

with

$$\mathbf{E} = \begin{bmatrix} 0 & -1 \\ 1 & 0 \end{bmatrix} \tag{6}$$

and ${}^b\mathbf{h}$ is the Cartesian coordinate vector of the MP Center of Mass (CoM) in $\mathscr{F}_b$ which is expressed as follows:

$${}^b\mathbf{h} = {}^b\mathbf{p} + {}^b\mathbf{R}_p {}^p\mathbf{h} \tag{7}$$

${}^p\mathbf{h} = \left[h_x, h_y \right]^T$ is the Cartesian coordinate vector of the CoM expressed in $\mathscr{F}_p$.

By considering $({}^b\mathbf{b}_i - {}^b\mathbf{p}) = {}^b\mathbf{R}_p {}^p\mathbf{b}_i$, $i = 1, 2, 3$, and $({}^b\mathbf{h} - {}^b\mathbf{p}) = {}^b\mathbf{R}_p {}^p\mathbf{h}$ we can rewrite Eq. (5) as follows:

$$\sum_{i=1}^{3} \left({}^p\mathbf{b}_i^T {}^b\mathbf{R}_p^T \mathbf{E}^T \mathbf{t}_i \right) + {}^p\mathbf{h}^T {}^b\mathbf{R}_p^T \mathbf{E}^T m\mathbf{g} = 0 \tag{8}$$

Finally, we write the equilibrium of the moments generated by cable loop about point P, the latter is the moment which drives Σ_2 and consequently actuates Σ_1 and is formulated as follows:

$$r_p \delta t + m_{fr} = 0 \tag{9}$$

r_p is the radius of the drum and cable loop tension difference is expressed in the following:

$$\delta t = t_2 - t_1 \tag{10}$$

From Eqs. (4), (8) and (9), the static equilibrium equation of the MP is expressed as:

$$\mathbf{W}\mathbf{t} + \mathbf{w}_e = \mathbf{0}_4 \tag{11}$$

where $\mathbf{W}$ is the wrench matrix of the CDPR under study

$$\mathbf{W} = \begin{bmatrix} {}^b\mathbf{u}_1 & {}^b\mathbf{u}_2 & {}^b\mathbf{u}_3 \\ {}^p\mathbf{b}_1^T {}^b\mathbf{R}_p^T \mathbf{E}^T {}^b\mathbf{u}_1 & {}^p\mathbf{b}_2^T {}^b\mathbf{R}_p^T \mathbf{E}^T {}^b\mathbf{u}_2 & {}^p\mathbf{b}_3^T {}^b\mathbf{R}_p^T \mathbf{E}^T {}^b\mathbf{u}_3 \\ -r_p & r_p & 0 \end{bmatrix} \tag{12}$$

$\mathbf{w}_e$ is the external wrench applied onto the MP

$$\mathbf{w}_e = [0 \quad -mg \quad {}^p\mathbf{h}^T {}^b\mathbf{R}_p^T \mathbf{E}^T m\mathbf{g} \quad m_{fr}]^T \tag{13}$$

$\mathbf{0}_4$ is a four dimensional zero vector and the three-dimensional cable tension vector, $\mathbf{t}$ is expressed as follows:

$$\mathbf{t} = [t_1 \quad t_2 \quad t_3]^T \tag{14}$$

4. Orientation of the Moving-Platform

Here, two methodologies for finding the orientation of MP are detailed. Two approaches calculate θ for a given position of point P. In the first approach, the orientation angle θ is computed based on loop closure equations (1) and static-equilibrium equation (11). The second approach aims at finding the orientation angle θ knowing the cable tension difference δt, and the Cartesian position coordinates of point P expressed in $\mathscr{F}_b$.

4.1. Orientation of the moving-platform obtained by Approach 1

In this section, the rotation angle θ of the MP is obtained while considering the three loop-closure equations defined by Eq. (1) and the static-equilibrium equations of the MP defined by Eq. (11). Accordingly, the following system of seven nonlinear equations with nine unknowns, i.e., θ, t_1, t_2, t_3, l_1, l_2,l_3, p_x and p_y is expressed:

$$\begin{cases} f_1(\theta, t_1, t_2, t_3, l_1, l_2, l_3, p_x, p_y) = 0 \\ f_2(\theta, t_1, t_2, t_3, l_1, l_2, l_3, p_x, p_y) = 0 \\ f_3(\theta, t_1, t_2, t_3, l_1, l_2, l_3, p_x, p_y) = 0 \\ f_4(\theta, t_1, t_2, t_3, l_1, l_2, l_3, p_x, p_y) = 0 \\ f_5(\theta, p_x, p_y) = 0 \\ f_6(\theta, p_x, p_y) = 0 \\ f_7(\theta, p_x, p_y) = 0 \end{cases} \tag{15}$$

f_1,f_2,f_3 and f_4 are obtained from Eq. (11) and they are functions of variables θ, t_1, t_2, t_3, l_1, l_2,l_3, p_x and p_y. The latter equations are expressed analytically as follows:

$$\begin{aligned} f_1 = {} & t_1 l_2 l_3 \left(a_{1x} - p_x - c_\theta b_{1x} + s_\theta b_{1y}\right) \\ & + t_2 l_1 l_3 \left(a_{2x} - p_x - c_\theta b_{2x} + s_\theta b_{2y}\right) \\ & + t_3 l_1 l_2 \left(a_{3x} - p_x - c_\theta b_{3x} + s_\theta b_{3y}\right) \end{aligned} \tag{16a}$$

$$\begin{aligned} f_2 = {} & t_1 l_2 l_3 \left(a_{1y} - p_y - s_\theta b_{1x} - c_\theta b_{1y}\right) \\ & + t_2 l_1 l_3 \left(a_{2y} - p_y - s_\theta b_{2x} - c_\theta b_{2y}\right) \\ & + t_3 l_1 l_2 \left(a_{3y} - p_y - s_\theta b_{3x} - c_\theta b_{3y}\right) - l_1 l_2 l_3 \; mg \end{aligned} \tag{16b}$$

$$\begin{aligned} f_3 = {} & t_1 l_2 l_3 \left(-s_\theta b_{1x} - c_\theta b_{1y}\right) \left(a_{1x} - p_x - c_\theta b_{1x} + s_\theta b_{1y}\right) \\ & + t_1 l_2 l_3 \left(c_\theta b_{1x} - s_\theta b_{1y}\right) \left(a_{1y} - p_y - s_\theta b_{1x} - c_\theta b_{1y}\right) \\ & + t_2 \, l_1 l_3 \left(-s_\theta b_{2x} - c_\theta b_{2y}\right) \left(a_{2x} - p_x - c_\theta b_{2x} + s_\theta b_{2y}\right) \\ & + t_2 \, l_1 l_3 \left(c_\theta b_{2x} - s_\theta b_{2y}\right) \left(a_{2y} - p_y - s_\theta b_{2x} - c_\theta b_{2y}\right) \\ & + t_3 l_1 l_2 \left(-s_\theta b_{3x} - c_\theta b_{3y}\right) \left(a_{3x} - p_x - c_\theta b_{3x} + s_\theta b_{3y}\right) \\ & + t_3 l_1 l_2 \left(c_\theta b_{3x} - s_\theta b_{3y}\right) \left(a_{3y} - p_y - s_\theta b_{3x} - c_\theta b_{3y}\right) \\ & - l_1 l_2 l_3 \; mg \left(h_x c_\theta - h_y s_\theta\right) \end{aligned} \tag{16c}$$

$$f_4 = (t_2 - t_1) r_p + m_{fr} \tag{16d}$$

where $s_\theta = \sin(\theta)$ and $c_\theta = \cos(\theta)$.

f_5, f_6 and f_7 are obtained from Eq. (1) and they are functions of variables θ, p_x and p_y. The latter equations are expressed analytically as follows:

$$f_5 = l_1^2 - \left(a_{1x} - p_x - c_\theta b_{1x} + s_\theta b_{1y}\right)^2 - \left(a_{1y} - p_y - s_\theta b_{1x} - c_\theta b_{1y}\right)^2 \tag{17a}$$

$$f_6 = l_2^2 - \left(a_{2x} - p_x - c_\theta b_{2x} + s_\theta b_{2y}\right)^2 - \left(a_{2y} - p_y - s_\theta b_{2x} - c_\theta b_{2y}\right)^2 \tag{17b}$$

$$f_7 = l_3^2 - \left(a_{3x} - p_x - c_\theta b_{3x} + s_\theta b_{3y}\right)^2 - \left(a_{3y} - p_y - s_\theta b_{3x} - c_\theta b_{3y}\right)^2 \tag{17c}$$

The under-determined system of non-linear equations (15) is studied for a given ${}^b\mathbf{p}$. As a result, a system consisting in seven equations and seven unknown is obtained. Hereafter, *lsqnonlin* ™Matlab function is used to solve this system of seven non-linear equations. It should be noted that the following constraints are taken into account for solving the system of equations in order to make sure that cable tensions are positive:

$$t_i > 0 \quad i = 1,\ 2,\ 3 \tag{18}$$

4.2. Orientation of the moving-platform obtained by Approach 2

This section presents a straightforward approach that enables us to obtain a sound approximation of the orientation of the MP without considering the geometrico-static model expressed in Eq. (11). This approach takes into account only the equilibrium of the moments applied/sustained about Instantaneous Center of Rotation (ICR) point regardless of the cables tension (t_1, t_2, t_3), but the difference of cable loop tensions, namely, δt.

The following equation expresses the equilibrium of the moments applied/sustained about ICR, point I, expressed in $\mathscr{F}_b$.

$$m_{12} + m_w = 0 \tag{19}$$

m_{12} is the moment applied onto the MP at point I due to cable tension difference δt. Then, moment m_{12} can be expressed as follows:

$$m_{12} = r_p \delta t \tag{20}$$

m_w is the moment applied onto the MP expressed at point I due to the MP weight, which is passing through point H.

$$m_w = ({}^b\mathbf{h} - {}^b\mathbf{i})^T \mathbf{E}^T m\mathbf{g} \tag{21}$$

under the assumption that segments A_1B_1 and A_2B_2 are parallel, which is valid as long as the MP is far from the points A_1 and A_2. In this approach the Cartesian coordinate vector point I, ${}^b\mathbf{i}$, is computed to formulate the pure rotation of the MP about this point.

ICR is the intersection point between the line $\mathcal{L}_{12}$ passing through points A_{12} and B_{12} and the line $\mathcal{L}_3$ passing through points A_3 and B_3. The equations of lines $\mathcal{L}_{12}$ and $\mathcal{L}_3$ are expressed as:

$$\mathcal{L}_{12}: \quad x(b_{12y} - a_{12y}) + y(a_{12x} - b_{12x}) - a_{12x}b_{12y} + a_{12y}b_{12x} = 0 \tag{22}$$

$$\mathcal{L}_3: \quad x(b_{3y} - a_{3y}) + y(a_{3x} - b_{3x}) - a_{3x}b_{3y} + a_{3y}b_{3x} = 0 \tag{23}$$

The Cartesian coordinate vector of points A_{12} and B_{12}, namely, ${}^b\mathbf{a}_{12} = [a_{12x},\ a_{12y}]^T$ and ${}^b\mathbf{b}_{12} = [b_{12x},\ b_{12y}]^T$ are the followings:

$${}^b\mathbf{a}_{12} = \frac{1}{2}({}^b\mathbf{a}_1 + {}^b\mathbf{a}_2) \tag{24}$$

$${}^b\mathbf{b}_{12} = \frac{1}{2}({}^b\mathbf{b}_1 + {}^b\mathbf{b}_2) = {}^b\mathbf{p} + \frac{1}{2}\,{}^b\mathbf{R}_p({}^p\mathbf{b}_1 + {}^p\mathbf{b}_2) \tag{25}$$

${}^b\mathbf{i}$ being the Cartesian coordinate vector of lines $\mathcal{L}_{12}$ and $\mathcal{L}_3$, i.e.,${}^b\mathbf{i} \equiv \mathcal{L}_{12} \cap \mathcal{L}_3$, the components of its Cartesian coordinate vector take the form:

$${}^b\mathbf{i} = [i_x,\ i_y]^T \tag{26}$$

with i_x and i_y being expressed as:

$$i_x = \frac{\mu_1\nu_2 - \mu_2\nu_1}{\lambda_1\mu_2 - \lambda_2\mu_1}, \quad i_y = \frac{-\nu_1 - \lambda_1 i_x}{\mu_1} \tag{27}$$

with

$$\begin{aligned} \lambda_1 &= \frac{1}{2}c_\theta(b_{1y} + b_{2y}) + \frac{1}{2}s_\theta(b_{1x} + b_{2x}) - \frac{1}{2}(a_{1y} - a_{2y}) + p_y \\ \lambda_2 &= b_{3x}s_\theta + b_{3y} - a_{3y}c_\theta - a_{3y} + p_y \\ \mu_1 &= -\frac{1}{2}c_\theta(b_{1x} + b_{2x}) + \frac{1}{2}s_\theta(b_{1y} + b_{2y}) + \frac{1}{2}(a_{1x} + a_{2x}) - p_x \\ \mu_2 &= b_{3y}s_\theta - b_{3x}c_\theta + a_{3x} - p_x \\ \nu_1 &= \frac{1}{4}c_\theta[(-a_{1x} - a_{2x})(b_{1y} + b_{2y}) + (b_{1x} + b_{2x})(a_{1y} + a_{2y})] \\ &\quad + \frac{1}{4}s_\theta[(-a_{1x} - a_{2x})(b_{1x} + b_{2x}) - (b_{1y} + b_{2y})(a_{1y} + a_{2y})] \\ &\quad - \frac{1}{2}p_y(a_{1x} - a_{2x}) + \frac{1}{2}p_x(a_{1y} - a_{2y}) \\ \nu_2 &= (a_{3y}b_{3x} - a_{3x}b_{3y})c_\theta - (a_{3x}b_{3x} + a_{3y}b_{3y})s_\theta - a_{3x}p_y + a_{3y}p_x \end{aligned} \tag{28}$$

In Fig. 3, all the relevant notations are illustrated. ICR point, I, is a function of θ, ${}^b\mathbf{p}$, ${}^b\mathbf{a}_i$ and ${}^p\mathbf{b}_i$, $i = 1,\ 2,\ 3$.
By using the following half tangent substitution in Eq. (29), Eq. (19) becomes the $6th$ order univariate polynomial equation (31).

$$\sin\theta = \frac{2t_\theta}{1+t_\theta^2},\quad \cos\theta = \frac{1-t_\theta^2}{1+t_\theta^2} \tag{29}$$

and,

$$t_\theta = \tan\frac{\theta}{2} \tag{30}$$

From Eqs. (26)-(30) we can rewrite Eq. (19) as follows:

$$C_6 t_\theta{}^6 + C_5 t_\theta{}^5 + C_4 t_\theta{}^4 + C_3 t_\theta{}^3 + C_2 t_\theta{}^2 + C_1 t_\theta + C_0 = 0 \tag{31}$$

Eq. (31) is a function of t_θ. The obtained polynomial is solved numerically to find t_θ. Then, θ can be substituted with t_θ based on Eq. (30). The coefficients of the latter polynomial, $C_0, C_1, ..., C_6$, are detailed in [1]. Equation (31) is solved in order to find the possible inclination(s) θ of the MP for a given position of its geometric center P.

5. Parasitic Inclinations

In this paper, parasitic inclination is defined as undesired orientation of the MP that leads to inaccuracy in manipulation and positioning. This kinematic situation is an outcome of utilizing cable loop in the CDPR. Since parasitic inclination decreases the accuracy of the robot, its investigation is crucial and can be employed to minimize the parasitic inclination by optimizing the design parameters in the design stage.
This section deals with the determination of the parasitic inclination, θ_p, of the MP due to cable tension differences, δt, into the cable-loop. Accordingly, the following methodology is defined:

1. To determine the natural inclination θ_n of the MP. θ_n amounts to the rotation angle θ of the MP obtained with both Approaches 1 and 2 described in Secs. 4.1 and 4.2, resp., for the same tensions in both strands $\mathscr{C}_1$ and $\mathscr{C}_2$ of the cable-loop, i.e., $\delta t = 0$.
2. To determine the inclination θ_m of the moving-platform when tensions in both strands of the cable-loop are not the same, i.e., $\delta t \neq 0$. θ_m can be also computed with Approaches 1 and 2 described in Secs. 4.1 and 4.2, respectively.
3. To determine the parasitic inclination, θ_p of the moving-platform. θ_p is the difference between θ_m and θ_n, i.e.,

$$\theta_p = \theta_m - \theta_n \tag{32}$$

6. Case study

The rotation angle θ and the parasitic inclination θ_p are computed in this section along a given path for the design parameters given in Tab. 1 of the four-DoF planar cable-driven parallel robot with a cable loop shown in Fig. 2. Eq. (33) expresses the Cartesian coordinates vector of seven via-points, namely, V_1,...,V_7, on the prescribed path (blue path in Fig. 2).

Table 1: CDPR Parameters associated to the case.

Anchor point coordinates [m]	Other parameters
${}^b\mathbf{a}_1 = [-2.03,\ 3]^T$	$m = 12$ [kg]
${}^b\mathbf{a}_2 = [-1.97,\ 3]^T$	$r_p = 0.03$ [m]
${}^b\mathbf{a}_3 = [2,\ 3]^T$	${}^p\mathbf{h} = [0,\ -0.3]^T$ [m]
${}^p\mathbf{b}_1 = [-0.28,\ 0.25]^T$	
${}^p\mathbf{b}_2 = [-0.22,\ 0.25]^T$	
${}^p\mathbf{b}_3 = [0.25,\ 0.25]^T$	

$$ {}^b\mathbf{v}_1 = \begin{bmatrix}-1\\0\end{bmatrix},\quad {}^b\mathbf{v}_2 = \begin{bmatrix}-1\\0.65\end{bmatrix}, {}^b\mathbf{v}_3 = \begin{bmatrix}-0.65\\+1\end{bmatrix},\quad {}^b\mathbf{v}_4 = \begin{bmatrix}0\\+1\end{bmatrix}$$

$$ {}^b\mathbf{v}_5 = \begin{bmatrix}0.65\\+1\end{bmatrix},\quad {}^b\mathbf{v}_6 = \begin{bmatrix}+1\\0.65\end{bmatrix}, {}^b\mathbf{v}_7 = \begin{bmatrix}+1\\0\end{bmatrix} \tag{33}$$

7. Discussion

Figure 4 shows the natural inclinations θ_{n1} and θ_{n2} of the previous case study obtained with approaches 1 and 2 along the prescribed path, respectively. The difference between θ_{n2} and θ_{n1} along the prescribed path is also depicted in Fig. 4. It appears that both approaches 1 and 2 give similar results, which confirms the soundness of the assumption made in approach 2. Figure 5 shows the rotation angle θ_{m1} and θ_{m2} of the moving-platform obtained with approaches 1 and 2, respectively, along the prescribed path, for $\delta t = 20$ N. Finally, Fig. 6 illustrates the parasitic inclination θ_p of the MP for different values of the cable tension difference δt into the cable-loop. It should be noted that θ_p increases with δt. This confirms the link between δt in the cable loop and the parasitic inclination of the MP.

Overall, the approach proposed in section 4.2 yields consistent results and can be applied to determine the parasitic inclination. Furthermore, this approach can be used to design the robot with respect to its parasitic inclination. This contributes to better control and more accurate positioning.

8. Conclusion

This paper introduced a four-DoF planar under-constrained cable-driven parallel robot. The robot utilizes a double-actuated cable loop system which grants an unlimited orientation workspace for the end-effector. Nevertheless, the moving-platform undergoes some parasitic inclinations that are due to the presence of a cable loop. Moreover, an analytical method to find the orientation of the moving-platform is presented. This method is validated by comparing its results with the solution of geometrico-static equations of the robot. Then, an approach was established to isolate the parasitic inclination induced by cable loop only from the natural inclination of the moving-platform.
Some experimental validations will be conducted in the future to validate the theoretical results presented in this paper. The optimim design paramerers of the robot will be also searched

[1] https://drive.google.com/file/d/0B80GqJ5822jObDlXNkdOUWd6UUE/view?usp=sharing

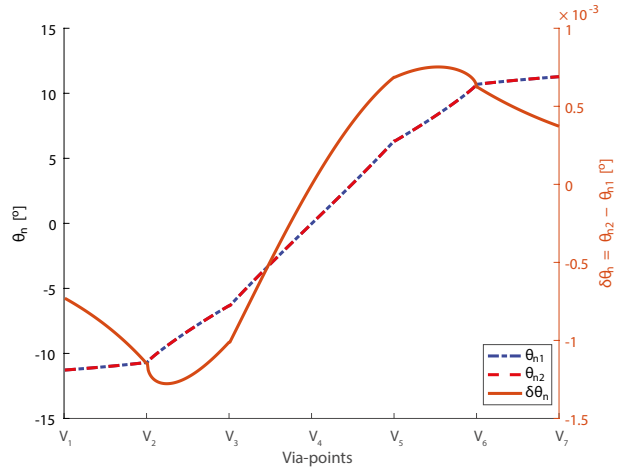

Fig. 4: Natural inclinations θ_{n1} and θ_{n2} of the moving-platform obtained with Approaches 1 and 2 along a prescribed path

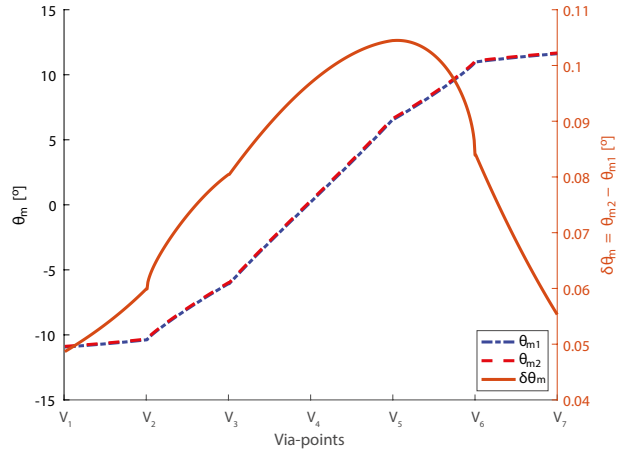

Fig. 5: Rotation angle θ_{m1} and θ_{m2} of the moving-platform obtained with Approaches 1 and 2 for δt = 20 N.

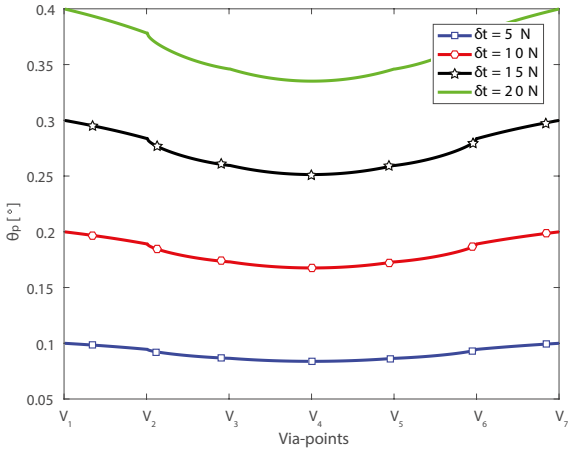

Fig. 6: Parasitic inclination θ_p of the moving-platform for different values of the cable tension difference δt into the cable-loop

for the parasitic inclinations of its articulated moving-platform to be a minimum.

References

[1] JA Carretero, RP Podhorodeski, MA Nahon, and Clement M Gosselin. Kinematic analysis and optimization of a new three degree-of-freedom spatial parallel manipulator. *Journal of mechanical design*, 122(1):17–24, 2000.

[2] Marco Carricato. Inverse geometrico-static problem of underconstrained cable-driven parallel robots with three cables. *Journal of Mechanisms and Robotics*, 5(3):031002, 2013.

[3] Lorenzo Gagliardini, Stéphane Caro, Marc Gouttefarde, and Alexis Girin. Discrete reconfiguration planning for cable-driven parallel robots. *Mechanism and Machine Theory*, 100:313–337, 2016.

[4] M John D Hayes and Robert G Langlois. Atlas motion platform: full-scale prototype. In *CSME International Congress*, 2012.

[5] M John D Hayes, Robert G Langlois, and Abraham Weiss. Atlas motion platform generalized kinematic model. *Meccanica*, 46(1):17–25, 2011.

[6] Jean-Baptiste Izard, Marc Gouttefarde, Micaël Michelin, Olivier Tempier, and Cedric Baradat. A reconfigurable robot for cable-driven parallel robotic research and industrial scenario proofing. In *Cable-driven parallel robots*, pages 135–148. Springer, 2013.

[7] Sadao Kawamura, Hitoshi Kino, and Choe Won. High-speed manipulation by using parallel wire-driven robots. *Robotica*, 18(1):13–21, 2000.

[8] Daniel Krebs, Gunnar Borchert, and Annika Raatz. Simulation and design of an orientation mechanism for assembly systems. *Procedia CIRP*, 44:245–250, 2016.

[9] Tam Nhat Le, Hiroki Dobashi, and Kiyoshi Nagai. Configuration of redundant drive wire mechanism using double actuator modules. *ROBOMECH Journal*, 3(1):25, 2016.

[10] Tam Nhat Le, Hiroki Dobashi, and Kiyoshi Nagai. Kinematical and static force analysis on redundant drive wire mechanism with velocity constraint modules to reduce the number of actuators. *ROBOMECH Journal*, 3(1):22, 2016.

[11] Rongfu Lin, Weizhong Guo, and Feng Gao. On parasitic motion of parallel mechanisms. In *ASME 2016 International Design Engineering Technical Conferences and Computers and Information in Engineering Conference*, pages V05BT07A077–V05BT07A077. American Society of Mechanical Engineers, 2016.

[12] Kiyoshi Nagai, Tam Nhat Le, Yoshikatsu Hayashi, and Koji Ito. Kinematical analysis of redundant drive wire mechanisms with velocity constraint. In *Mechatronics and Automation (ICMA), 2012 International Conference on*, pages 1496–1501. IEEE, 2012.

[13] Dinh Quan Nguyen, Marc Gouttefarde, Olivier Company, and Francois Pierrot. On the analysis of large-dimension reconfigurable suspended cable-driven parallel robots. In *Robotics and Automation (ICRA), 2014 IEEE International Conference on*, pages 5728–5735. IEEE, 2014.

[14] Angelos Platis, Tahir Rasheed, Philippe Cardou, and Stéphane Caro. Isotropic design of the spherical wrist of a cable-driven parallel robot. In *Advances in Robot Kinematics 2016*, pages 321–330. Springer, 2018.

[15] Giulio Rosati, Damiano Zanotto, and Sunil K Agrawal. On the design of adaptive cable-driven systems. *Journal of mechanisms and robotics*, 3(2):021004, 2011.

[16] Xiaoqiang Tang and Rui Yao. Dimensional design on the six-cable driven parallel manipulator of fast. *Journal of Mechanical Design*, 133(11):111012, 2011.